THE JOURNAL OF BIOLOGICAL CHEMISTRY VOL. 286, NO. 39, pp. 33854–33862, September 30, 2011

EPI64 Protein Functions as a Physiological GTPase-activating Protein for Rab27 Protein and Regulates Amylase Release in Rat Parotid Acinar Cells*[S]

Received for publication, July 10, 2011, and in revised form, August 3, 2011 Published, JBC Papers in Press, August 5, 2011, DOI 10.1074/jbc.M111.281394

Akane Imai[‡1], Sumio Yoshie[§], Koutaro Ishibashi[¶], Maiko Haga-Tsujimura[§], Tomoko Nashida[‡], Hiromi Shimomura[‡], and Mitsunori Fukuda[¶2]

From the Departments of [‡]Biochemistry and [§]Histology, The Nippon Dental University, School of Life Dentistry at Niigata, 1-8 Hamaura-cho, Chuo-ku, Niigata 951-8580, Japan and the [¶]Laboratory of Membrane Trafficking Mechanisms, Department of Developmental Biology and Neurosciences, Graduate School of Life Sciences, Tohoku University, Aobayama, Aoba-ku, Sendai, Miyagi 980-8578, Japan

Rab27, a small GTPase, is generally recognized as an important regulator of secretion that interacts with Rab27-specific effectors to regulate events in a wide variety of cells, including endocrine and exocrine cells. However, the mechanisms governing the spatio-temporal regulation of GTPase activity of Rab27 are not firmly established, and no GTPase-activating protein (GAP) specific for Rab27 has been identified in secretory cells. We previously showed that expression of EPI64, a Tre-2/Bub2/Cdc16 (TBC)-domain-containing protein, in melanocytes inactivates endogenous Rab27A on melanosomes (Itoh, T., and Fukuda, M. (2006) *J. Biol. Chem.* 281, 31823–31831), but the EPI64 role in secretory cells has never been investigated. In this study, we investigated the effect of EPI64 on Rab27 in isoproterenol (IPR)-stimulated amylase release from rat parotid acinar cells. Subcellular fractionation and immunohistochemical analyses indicated that EPI64 was enriched on the apical plasma membrane of parotid acinar cells. We found that an antibody against the TBC/Rab-GAP domain of EPI64 inhibited the reduction in levels of the endogenous GTP-Rab27 in streptolysin-O-permeabilized parotid acinar cells and suppressed amylase release in a dose-dependent manner. We also found that the levels of *EPI64* mRNA and EPI64 protein increased after IPR stimulation, and that treatment with actinomycin D or antisense-*EPI64* oligonucleotides suppressed the increase of *EPI64* mRNA/EPI64 protein and the amount of amylase released. Our findings indicated that EPI64 acted as a physiological Rab27-GAP that enhanced GTPase activity of Rab27 in response to IPR stimulation, and that this activity is required for IPR-induced amylase release.

Small GTPase Rabs are believed to play important roles in intracellular membrane trafficking (reviewed in Refs. 1–4). More than 60 distinct Rab isoforms have been identified in humans and mice, and these proteins form a large subfamily of the small GTPase superfamily (5–7). Rab activity is regulated by the GDP/GTP cycle (1–4, 8), with GTP-Rab and GDP-Rab representing active and inactive forms, respectively. Distinct individual Rabs interact with a specific effector/regulator, and these complexes regulate different steps of membrane trafficking in cells, and they function as either an accelerator or a brake (9, 10). GTP bound to a particular Rab is hydrolyzed by intrinsic GTPase activity, and this activity is enhanced by a specific GTPase-activating protein (GAP)[3] (11).

The TBC (Tre-2/Bub2/Cdc16) domain is a conserved protein motif with ~200 amino acids and is known to be present in a variety of molecules in eukaryotic organisms (12). Because the TBC domain of yeast, Gyps (GAP for Ypt proteins), has been shown to function as a GAP domain for small GTPase Ypt/Rab, TBC domain-containing proteins (referred to as TBC proteins hereafter) in other species are also expected to function as specific Rab-GAPs. Humans and mice each have more than 40 TBC proteins, and substantial evidence has accumulated recently indicating that some mammalian TBC domains function as a GAP domain for the Rab family small GTPases (11, 12) (see also Table in Ref. 13). However, since the GAP activity of most of the mammalian TBC proteins has been determined by *in vitro* GAP assays or by forced overexpression of TBC proteins in cultured cells, little is known about the Rab-GAP function of "endogenous" TBC proteins in mammalian cells.

Previously, we identified a TBC protein, EPI64, as a candidate GAP specific for Rab27; Rab27 regulates a variety of secretion

* This work was supported in part by Grants-in-Aid for Scientific Research from the Ministry of Education, Culture, Sports, Science, and Technology (MEXT) of Japan (to A. I. and M. F.), by a Research Promotion Grant (NDUF-10-03 and 11-10; to A. I.) from The Nippon Dental University, and by a grant from the Global Center of Excellence (GCOE) Program (Basic & Translational Research Center for Global Brain Science) from MEXT of Japan (to M. F.). Supported was also provided by the Japan Society for the Promotion of Science (to K. I.).

[S] The on-line version of this article (available at http://www.jbc.org) contains supplemental Figs. S1–S3.

[1] To whom correspondence may be addressed: Dept. of Biochemistry, School of Life Dentistry at Niigata, The Nippon Dental University, 1-8 Hamaura-cho, Chuo-ku, Niigata 951-8580, Japan. Tel.: 81-25-267-1500; Fax: 81-25-267-1134; E-mail: imaiak@ngt.ndu.ac.jp.

[2] To whom correspondence may be addressed: Laboratory of Membrane Trafficking Mechanisms, Dept. of Developmental Biology and Neurosciences, Graduate School of Life Sciences, Tohoku University, Aobayama, Aoba-ku, Sendai, Miyagi 980-8578, Japan. Tel.: 81-22-795-7731; Fax: 81-22-795-7733; E-mail: nori@m.tohoku.ac.jp.

[3] The abbreviations used are: GAP, GTPase-activating protein; APM, apical plasma membrane; AQP5, aquaporin 5; BLM, basolateral plasma membrane; EPI64, EBP50-PDZ interactor of 64 kD; IgG, immunoglobulin G; IPR, isoproterenol; LNA, locked nucleic acid; RBD35, Rab-binding domain specific for Rab35; RT, reverse transcription; SGM, secretory granule membrane; SHD, synaptotagmin-like protein homology domain; SLO, streptolysin O; TBC, Tre-2/Bub2/Cdc16.

events in secretory cells and melanosome transport in melanocytes (reviewed in Ref. 14). EPI64 (also called TBC1D10A/Rab27A-GAPα) was originally described as an EBP50-binding protein (EBP50-PDZ interactor of 64 kDa) involved in microvillar formation (15, 16). We showed that overexpression of EPI64 in cultured melanocytes caused dissociation of endogenous Rab27A from mature melanosomes and induced peri-nuclear aggregation of melanosomes as a result of the Rab27A inactivation (17). However, we have not determined whether endogenous EPI64 protein functions as a Rab27-GAP in melanocytes or secretory cells under physiological conditions.

In the present study, we investigated the subcellular localization and Rab27-GAP function of EPI64 in regulated secretion using isoproterenol (IPR)-induced amylase release from rat parotid acinar cells as a secretion model. We showed that EPI64 enhanced the GTPase activity of Rab27 in response to IPR stimulation, and that Rab27-GAP activity is required for IPR-induced amylase release. We further found that both *EPI64* mRNA and EPI64 protein levels increased following IPR stimulation. Based on these findings, we discuss the possible regulatory mechanism of EPI64 during IPR-induced amylase release from parotid acinar cells.

EXPERIMENTAL PROCEDURES

Materials—Anti-EPI64-C and anti-EPI64-TBC antibodies were generated by immunizing New Zealand White rabbits with a C-terminal peptide (CAHHRSQESLTSQESEDTYL; an artificial Cys residue is added to the N terminus for conjugation of the peptide with keyhole limpet hemocyanin) and a TBC-domain peptide (CGKVKLQQNPGKFDE), respectively, of human EPI64. Each antibody was partially purified by ammonium sulfate fractionation as described previously (18) and then affinity-purified by exposure to antigenic peptide bound to FMP activated-cellulofine beads according to the manufacturer's instructions (Seikagaku Co., Tokyo, Japan). Anti-Rab27A/B and anti-aquaporin 5 (AQP5) rabbit polyclonal antibodies were purchased from Immuno-Biological Laboratories Ltd. (Takasaki, Japan) and Millipore (Billerica, MA), respectively. Anti-Rab27A and anti-vesicle-associated membrane protein-2 (VAMP-2) mouse monoclonal antibodies were obtained from Abcam (Cambridge, UK) and Synaptic Systems (Göttingen, Germany), respectively. Anti-GDI rabbit polyclonal antibody was obtained from Zymed Laboratories Inc. (San Francisco, CA). Anti-Noc2 rabbit polyclonal antibody was prepared as described previously (19). Horseradish peroxidase-conjugated anti-T7 tag mouse monoclonal antibody was purchased from Merck Biosciences Novagen (Darmstadt, Germany). Actinomycin D, PCR primers, and other chemical products were purchased from Sigma-Aldrich. Protein kinase A inhibitor 5–24 was from Calbiochem Merck KGaA (Darmstadt, Germany). Rat tissue cDNA QUICK-clone was from TAKARA Bio Inc. (Kyoto, Japan). Locked nucleic acid (LNA) antisense oligonucleotides (20), corresponding to rat EPI64 (5′-TCCTGGGAGCAAGAGCATA-3′) (*EPI64* antisense LNA), were provided by GeneDesign Inc. (Osaka, Japan).

Preparation of Total RNA and Subcellular Fractionation of Parotid Acinar Cells—All animal protocols were devised and performed in accordance with the Guidelines of the Nippon Dental University for the Care and Use of Laboratory Animals. Parotid acinar cells were prepared from parotid glands of male Wistar rats (~10 weeks old) by enzyme digestion using trypsin (Sigma-Aldrich) and collagenase (CLSPA; Worthington Biochemical Co., Lakewood, NJ) as described previously (21). Total RNA from parotid acinar cells was prepared with an RNeasy Plus Mini kit (Qiagen GmbH, Hilden, Germany) according to the manufacturer's instructions. Subcellular fractions were prepared from the homogenate of the acinar cells as described previously (22). Specifically, parotid acinar cells were homogenized in a 20-fold volume of buffer A (5 mM HEPES-NaOH buffer (pH 7.2) containing 50 mM mannitol, 0.25 mM $MgCl_2$, 25 mM β-mercaptoethanol, 0.1 mM EGTA, 2 μM leupeptin, 2.5 μg/ml trypsin inhibitor, 0.1 mM 4-amidinophenylmethanesulphonyl fluoride hydrochloride (*p*-APMSF), 5 mM benzamidine, and 2 μg/ml aprotinin) using a glass homogenizer with a Teflon pestle. Homogenate was centrifuged at 9,750 $\times$ *g* for 10 min at 4 °C. Supernatant was then re-centrifuged at 35,000 $\times$ *g* for 30 min at 4 °C, and further centrifuged at 100,000 $\times$ *g* for 1 h. The precipitate was the intracellular membrane (ICM) fraction, and the supernatant was the cytosolic (Cyto) fraction. The 35,000 $\times$ *g* pellet was suspended in buffer A containing 10 mM $MgCl_2$ and left on ice for 30 min. The suspension was centrifuged at 3,000 $\times$ *g* for 15 min, and the resultant precipitate was obtained as the basolateral plasma membrane (BLM) fraction. The resultant supernatant was re-centrifuged at 100,000 $\times$ *g* for 1 h, and the resultant precipitate was recovered as the apical plasma membrane (APM) fraction. The APM and BLM fractions were characterized by specific enzyme activities, γ-glutamyl transpeptidase activity for the APM, and K^+-stimulated *p*-nitrophenyl-phosphatase activity for the BLM (23, 24). A secretory granule membrane (SGM) fraction was prepared by centrifugation in 40% Percoll gradient (25). Protein assays were performed using a protein assay kit (Bio-Rad).

IPR Stimulation of Parotid Acinar Cells—Suspensions of parotid acinar cells or slices <1 mm^3 in volume were equally divided into three tubes. Preincubation was performed at 37 °C for 10 min in 5 ml of Hanks' balanced salt solution containing 0.5% bovine serum albumin. The cells or slices were then stimulated with 1 μM IPR for 0, 5, or 30 min. After incubation, the medium was immediately removed by centrifugation at 500 $\times$ *g* for 1 min at 4 °C. Acinar cells were washed twice with ice-cold homogenization buffer A and subjected to preparation of total RNA and subcellular fractions. Parotid slices were used for immunohistochemistry as described below.

Immunoblotting—Sodium dodecyl sulfate-polyacrylamide gel electrophoresis (SDS-PAGE) and immunoblot analysis were performed as described previously (26). Samples were separated by 10% SDS-PAGE. Proteins in the gel were transferred to Immun-Blot PVDF membranes (Bio-Rad) using a semi-dry blotter. Membranes were probed with anti-EPI64-C polyclonal antibody (1/500 dilution) or anti-Rab27 polyclonal antibody (1/250 dilution). Membranes were washed and then incubated with anti-rabbit immunoglobulin G (IgG) horseradish peroxidase-conjugated secondary antibody (Sigma-Aldrich) (1/3000 dilution), followed again by washing. Immunoreactive bands were visualized using an ECL or ECL plus detection system (GE Healthcare Biosciences, Piscataway, NJ) according to the man-

ufacturer's instructions. The intensity of immunoreactive bands on a film was quantified using Image Gauge (LAS-1000 software; Fuji Film, Tokyo, Japan).

Reverse Transcription (RT)-PCR and Real-time PCR—Parotid cDNA was prepared from total RNA of rat parotid acinar cells, and cDNA from other tissue was made using the QUICK-clone system. Reverse transcription of total RNA from parotid acinar cells was performed using a Transcriptor First Strand cDNA Synthesis kit (Roche, Basel, Switzerland). Synthesized cDNA was made from 1 μg of the total RNA preparation, and 1/20 of the reverse transcriptase reaction mix was used for PCR or quantitative real-time PCR. PCR was performed with KOD-plus DNA polymerase (TOYOBO, Osaka, Japan) and specific primers corresponding to rat *EPI64* (forward: 5′-CAGAATC-CTGGAAAATTTGAT-3′; and reverse: 5′-TGGATTGCCTC-CAGTTTCTC-3′) and glyceraldehyde 3-phosphate dehydrogenase (GAPDH) (forward: 5′-AACATCATCCCTGCATCC-AC-3′; and reverse: 5′-GACAACCTGGTCCTCAG-TGT-3′). Real-time PCR was carried out using a LightCycler Carousel-Based System (Roche). A TaqMan Master kit (Roche) with Universal Probe Library (Roche) was used to evaluate gene expression of *EPI64,* as a target, and TaqMan Gene Expression Assays (Assay ID, Rn99999916_s1, Applied Biosystems) was used to evaluate gene expression of *GAPDH,* as a reference, in parotid acinar cells. PCR primers and probe (#65) for *EPI64* (Tbc1d10a: NM_001015022.3) were designed with the Probe Library Assay Design Center. *EPI64* expression by real-time PCR was normalized to *GAPDH*, an endogenous control. Rat brain cDNA (QUICK-clone) was used as a standard.

Amylase Release from Permeabilized Parotid Acinar Cells—Amylase release from streptolysin O (SLO)-permeabilized acinar cells was measured as described previously (26). Lyophilized SLO powder (Sigma-Aldrich) was dissolved in 10 mM PBS (pH 7.0) and was activated with 10 mM dithiothreitol for 1 h at 0 °C. Parotid acinar cells were washed twice with incubation medium (20 mM HEPES-NaOH (pH 7.2), 140 mM KCl, 1 mM $MgSO_4$, 1 mM Mg-ATP, 0.1 mg/ml trypsin inhibitor, and 0.1% bovine serum albumin). The effect of the anti-EPI64-TBC IgG on IPR-induced amylase release was investigated as follows. The cell suspension (100 μl) was pipetted into a tube containing 2 μl of 2500 units/ml SLO together with either anti-EPI64-TBC IgG, normal rabbit IgG, or *EPI64* antisense LNA, and incubated at 37 °C for 5 min (for IgG) or 30 min (for antisense LNA). The suspension was then stimulated with 1 μM IPR for 20 min. The reaction mixture was added to 900 μl of incubation medium, and was immediately filtered through glass filter paper to remove acinar cells, and the filtrate, containing released amylase, was used for the amylase assay. Total amylase activity was assayed from centrifuged supernatant after acinar cells were homogenized in 0.1% Triton X-100. Amylase activity was measured as described by Bernfeld (27). Namely, the activities were indicated by the amount of maltose that was produced from starch. Amylase release of 100% was represented as the differential amylase activities with and without IPR stimulation under control conditions. Approximately 5% of the total amylase was released by IPR stimulation under our experimental conditions. To evaluate the effect of actinomycin D on IPR-induced amylase release, we also prepared a saponin-permeabilized cell suspension (28) and measured amylase release in the presence of actinomycin D, and without antibody or antisense LNA, as described above.

GTP-Rab27 Pull-down Assay with Glutathione S-Transferase (GST)-Synaptotagmin-like Protein Homology Domain (SHD) of Slac2-b—The amount of GTP-Rab27 in parotid acinar cells was measured by affinity pull-down using the Slac2-b SHD as described previously (29). Briefly, anti-EPI64-TBC IgG or control rabbit IgG was introduced into the SLO-permeabilized parotid acinar cells. The cells were incubated for 20 min and then stimulated with 1 μM IPR for 20 min. Membrane-associated proteins, including Rab27, were solubilized in buffer B (50 mM HEPES-KOH (pH 7.2), 80 mM KCl, 4 mM $MgCl_2$, 0.2 mM $CaCl_2$, 2 mM EGTA, 1 mM dithiothreitol, 2 μM leupeptin, 2.5 μg/ml trypsin inhibitor, 0.1 mM *p*-APMSF, 5 mM benzamidine, and 2 μg/ml aprotinin) containing 0.5% Triton X-100 at 4 °C for 5 min followed by centrifugation at 100,000 $\times$ *g* for 10 min. Supernatants were incubated with glutathione-Sepharose beads (GE Healthcare Biosciences) coated with 10 μg of the GST fusion protein with the SHD from Slac2-b (simply referred to as GST-SHD hereafter) at 4 °C for 30 min. The beads were washed four times with buffer B containing 0.1% Triton X-100 and boiled in Laemmli SDS-sample buffer for elution. GTP-Rab27 proteins bound to the beads were analyzed by immunoblotting with anti-Rab27 antibody as described above. GTP-Rab35 pull-down assay was similarly performed by using a specific Rab35 trapper, GST-RBD35 (Rab-binding domain specific for Rab35), that was recently developed (30).

Immunoprecipitation—Homogenate (500 μg of protein) of parotid acinar cells was solubilized with 1% Triton X-100 at 4 °C for 1 h. Insoluble materials were removed by centrifugation at 15,000 $\times$ *g* for 10 min. Supernatant was incubated with anti-EPI64-C IgG (10 μg/ml) at 4 °C for 1 h and with Dynabeads M-280 sheep anti-rabbit IgG (Dynal Biotech, Oslo, Norway) for 1 h at 4 °C. After washing the beads five times with 50 mM HEPES-KOH (pH 7.2), 150 mM NaCl, and 0.5% Triton X-100, the beads were boiled in Laemmli SDS-sample buffer. Immnoblotting was performed as described above.

Immunohistochemistry—IPR-stimulated parotid slices were immediately fixed with 4% (w/v) paraformaldehyde dissolved in 0.07 M phosphate buffer (pH 7.3) for 8 h at room temperature. Fixed specimens were then rapidly frozen in isopentane precooled to −35 °C. Frozen sections (6 μm) were cut using a cryostat, mounted on APS-coated glass slides (Matsunami Glass, Osaka, Japan), and processed for the following immunostaining procedures. Since both anti-EPI64-TBC and anti-AQP5 polyclonal antibodies were prepared from rabbits, we used a Zenon Rabbit IgG Labeling kit (Molecular Probes, Eugene, OR) for double immunostaining. The sections were incubated for 1–2 h at room temperature with diluted Zenon labeling complexes (Alexa Fluor 488-labeled anti-EPI64-TBC rabbit IgG: 1/200 dilution; Alexa Fluor 594-labeled anti-AQP5 rabbit IgG: 1/200 dilution) and treated as described in the manufacturer's instructions. The other sections were co-immunostained with anti-EPI64-TBC rabbit antibody and anti-Rab27A (1/200 dilution) mouse monoclonal antibody followed by exposure to Alexa Fluor 488- and 594-labeled secondary antibodies (each 1/100 dilution), respectively. Stained sections were examined

and photographed under a confocal laser scanning microscope (LSM 710; Carl Zeiss, Göttingen, Germany).

Treatment of Parotid Acinar Cells with Actinomycin D or EPI64 Antisense LNA—Parotid acinar cells were washed twice with incubation medium (20 mM HEPES-NaOH (pH 7.2), 140 mM KCl, 1 mM $MgSO_4$, 1 mM Mg-ATP, 0.1 mg/ml trypsin inhibitor, and 0.1% bovine serum albumin). The effects of actinomycin D or *EPI64* antisense LNA on IPR-induced up-regulation of *EPI64* mRNA and EPI64 protein were investigated as follows. The cell suspension (100 μl) was pipetted into a tube containing 2 μl of 2500 units/ml SLO together with *EPI64* antisense LNA (final concentration; 50 nM), or 2 μl of 1 mg/ml saponin together with actinomycin D (final concentration; 50 μg/ml) and incubated at 37 °C for 20 min. The cell suspensions were then stimulated with 1 μM IPR for 30 min. After the stimulation, the cells were collected by centrifugation at 90 × *g* for 10 min, resuspended in 100 μl of RNA*later* (Ambion, Austin, TX) (or homogenization buffer A) on ice, and subjected to preparation of total RNA for RT-PCR analysis (or homogenate for SDS-PAGE) as described above.

RESULTS

Expression and Subcellular Localization of EPI64 in Parotid Acinar Cells—We previously showed that EPI64 is a candidate Rab27-GAP, because its overexpression in melanocytes caused inactivation of endogenous Rab27A molecules (17). To determine whether EPI64 actually functions as a physiological Rab27-GAP, we chose amylase release from parotid acinar cells as a secretion model for the following reasons. First, parotid acinar cells are typical exocrine cells that contain many secretory granules to which both Rab27A and Rab27B are localized (31). These secretory granules undergo exocytosis in response to IPR, a β-adrenergic stimulant (32–34), and their contents, including amylase, are released. Functional blocking of Rab27 either with a specific antibody or by a specific Rab27 trapper (*i.e.* GST-SHD (29, 35)) causes a reduction in the amount of amylase release (31). Second, Rab27 effectors (*e.g.* Slp4-a/granuphilin-a, Slac2-c/MyRIP, and Noc2) that regulate Rab27 in parotid acinar cells have been identified, and blocking the function of these effectors also reduces amylase release (36–38). Third, the behavior and the recycling of Rab27 proteins after IPR stimulation is well documented in parotid acinar cells (22). For the most part, GTP-Rab27 is present on secretory granules under resting conditions, and it translocates to the apical plasma membrane (APM) 5 min after IPR stimulation. GTP-Rab27 is then inactivated and dissociation of the resulting GDP-Rab from the APM is mediated by the activity of a Rab-specific GDP dissociation inhibitor during 30 min after IPR stimulation. We therefore think that amylase release from parotid acinar cells is an ideal system in which to investigate the involvement of EPI64 in the conversion of GTP-Rab27 to GDP-Rab27 after IPR stimulation.

We first examined the expression of *EPI64* mRNA in rat parotid acinar cells by RT-PCR analysis. As shown in Fig. 1*A*, *EPI64* mRNA was detected in parotid acinar cells and in all tissues tested. We then generated two anti-EPI64 antibodies (anti-EPI64-C antibody and anti-EPI64-TBC antibody) to assess the expression of EPI64 protein in parotid acinar cells. The specificity of each antibody was assessed by immunoblotting with recombinant T7-tagged TBC1D10 family members expressed in COS-7 cells (Fig. 1*B*). Notably, both antibodies specifically recognized EPI64/TBC1D10A (*lanes 1* and *4* in Fig. 1*B*), but not two closely related proteins, TBC1D10B and TBC1D10C/EPI64C (13, 39, 40). We then analyzed the EPI64 protein expression in rat parotid glands by immunoblotting with anti-EPI64-C antibody (Fig. 1*C*). Consistent with the results of the RT-PCR analysis, EPI64 was detected in all tissues tested, but a high level of EPI64 expression was observed in the kidney.

We further investigated the subcellular distribution of EPI64 in parotid acinar cells by subcellular fractionation (Fig. 1*D*). Parotid acinar cells are typical exocrine cells and can be separated into five different fractions, *i.e.* basolateral plasma membrane (BLM), apical plasma membrane (APM), intracellular membrane (ICM), secretory granule membrane (SGM), and cytosol (Cyto), by ultracentrifugation (22) (see "Experimental Procedures" for details). Interestingly, EPI64 protein had a polarized distribution in parotid acinar cells. It was enriched in the APM, where Rab27-bearing secretory granules are known to fuse (31), and some EPI64 signal was also present in the cytosolic fraction (*lanes 2* and *5* in Fig. 1*D*).

Inhibition of Amylase Release by Anti-EPI64-TBC IgG—To investigate the involvement of EPI64 in IPR-induced amylase release from parotid acinar cells, we tested the effect of antibody against the TBC/Rab-GAP domain (anti-EPI64-TBC) on IPR-induced amylase release from SLO-permeabilized parotid acinar cells (Fig. 2). Interestingly, introduction of the anti-EPI64-TBC IgG into SLO-permeabilized parotid acinar cells caused a reduction in IPR-induced amylase release in a dose-dependent manner (up to ~50% of control IPR-induced amylase release) (*closed diamonds* in Fig. 2). By contrast, control rabbit IgG had no effect on IPR-induced amylase release under the same experimental conditions (*open squares* in Fig. 2).

Effect of Anti-EPI64-TBC IgG on the GTP Binding Status of Rab27—If EPI64 actually functions as Rab27-GAP during IPR-induced amylase release under physiological conditions, anti-EPI64-TBC IgG should affect the GTP binding status of Rab27. Therefore, we measured the amount of endogenous GTP-Rab27 in SLO-permeabilized parotid acinar cells with or without anti-EPI64-TBC IgG treatment using a GTP-Rab27 pull-down assay with a GST-SHD bait (29, 35) (Fig. 3*A*). The results of the pull-down assay clearly indicated that the amount of endogenous GTP-Rab27 was significantly decreased in response to IPR stimulation under control conditions (~50% of the unstimulated conditions; compare *lane 1* with *lanes 3/5* in Fig. 3*B*), whereas anti-EPI64-TBC IgG completely inhibited the reduction of GTP-Rab27 to the level before the stimulation (*lane 4* in Fig. 3*B*). Based on this result, we concluded that the anti-EPI64-TBC IgG inhibited the GAP activity of endogenous EPI64 molecules, which in turn inhibited the reduction of GTP-Rab27 following IPR stimulation.

Furthermore, EPI64 and its substrate Rab27 were co-localized at the luminal sites of parotid acinar cells before and after IPR stimulation (Fig. 4*B*), and the EPI64/Rab27A complex was also detected before and after IPR stimulation (Fig. 4*A* and data

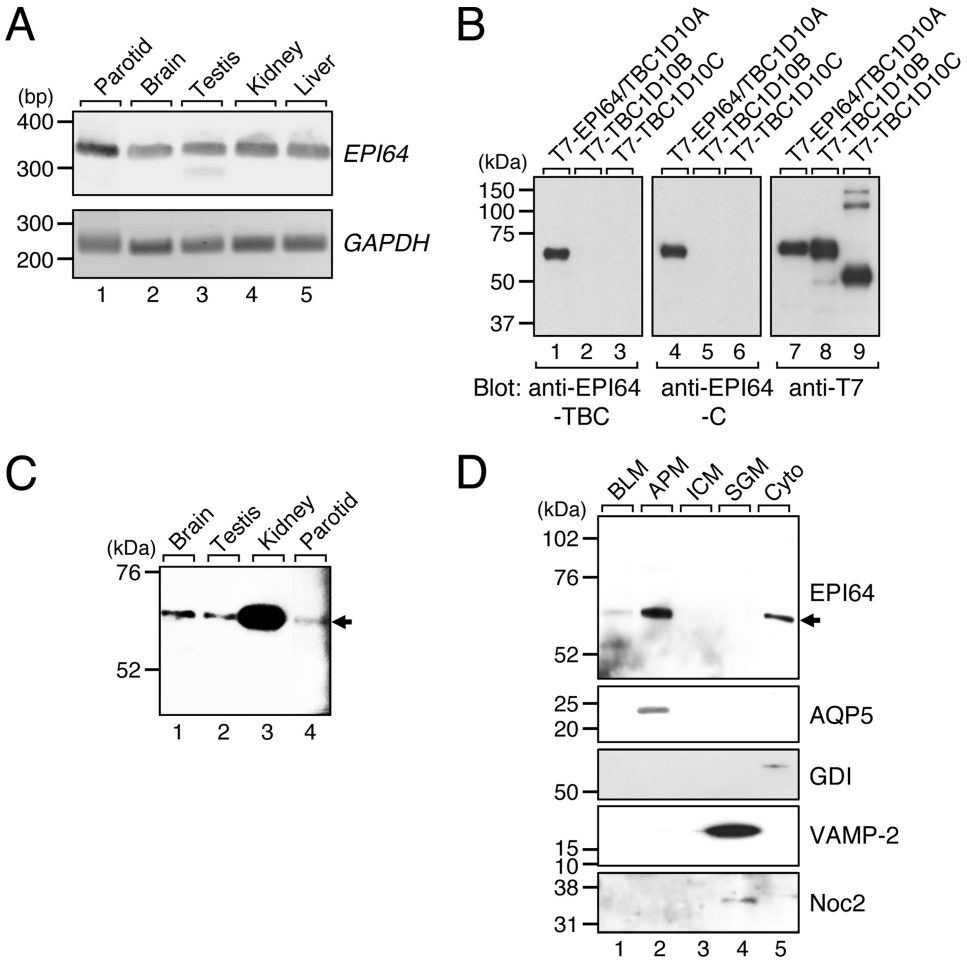

FIGURE 1. **Expression and subcellular localization of EPI64 in rat parotid gland.** *A*, mRNA expression of *EPI64* in parotid acinar cells (Parotid), brain, testis, kidney, and liver as revealed by RT-PCR analysis. *GAPDH*, a housekeeping gene, was used as a positive control for mRNA. RT-PCR products were detected as 319-bp and 237-bp bands for *EPI64* and *GAPDH*, respectively. *EPI64* mRNA was detected in parotid acinar cells and all other tissues. The size of the molecular weight markers (*bp*, base pair) is shown at the left. *B*, specificity of anti-EPI64 rabbit polyclonal antibodies (anti-EPI64-TBC and anti-EPI64-C) used in this study. Recombinant T7-tagged EPI64/TBC1D10A (*lanes 1*, *4*, and *7*), TBC1D10B (*lanes 2*, *5*, and *8*), and TBC1D10C (*lanes 3*, *6*, and *9*) were subjected to 10% SDS-PAGE followed by immunoblotting with anti-EPI64-TBC antibody (*lanes 1–3*), anti-EPI64-C antibody (*lanes 4–6*), or anti-T7 tag antibody (*lanes 7–9*). Note that both antibodies against EPI64 specifically recognized EPI64/TBC1D10A (*lanes 1* and *4*). The positions of the molecular mass markers (M_r in kilodaltons) are shown on the *left*. *C*, rat brain, testis, kidney, and parotid lysates (each 5 μg of protein) were separated by 10% SDS-PAGE and analyzed by immunoblotting with anti-EPI64-C antibody. EPI64 protein was detected in parotid acinar cells (*lane 4*, *arrow*) and all other tissues. The positions of the molecular mass markers (M_r in kilodaltons) are shown on the *left*. *D*, subcellular localization of EPI64 in rat parotid acinar cells. Lanes are *BLM*, basolateral plasma membrane; *APM*, apical plasma membrane; *ICM*, intracellular membrane; *SGM*, secretory granule membrane; and *Cyto*, cytosolic fractions. They (each 5 μg of protein) were processed as described under "Experimental Procedures," and proper fractionations were confirmed by immunoblotting with antibodies against several fractionation markers, including AQP5 (a marker for the APM), VAMP-2, and Noc2 (markers for the SGM), and GDI (GDP dissociation inhibitor, a marker for the Cyto). Note that EPI64 was enriched at the APM fraction (*lane 2*) and that some portions of EPI64 were also present in the cytosolic fraction (*lane 5*). The positions of the molecular mass markers (M_r in kilodaltons) are shown on the *left*.

not shown) by co-immunoprecipitation assays. These results also supported our conclusion that EPI64 functions as a Rab27-GAP in parotid acinar cells.

Redistribution and Increased Protein Expression of EPI64 in Parotid Acinar Cells after IPR Stimulation—Although the EPI64 protein was predominantly localized at the APM of parotid acinar cells under resting conditions, the subcellular localization of EPI64 may change following IPR stimulation, as does Rab27 distribution (from secretory granules to the APM, and then to the cytosol) in response to stimuli (22). To investigate this possibility, we performed an immunohistochemical analysis with the anti-EPI64-TBC antibody. Parotid slices were incubated with 1 μM IPR for 5 min or 30 min, and each section was immunostained with anti-EPI64-TBC antibody or anti-AQP5 antibody (a marker for the APM (41)) (Fig. 5*A*, *panels a–i*). Although EPI64 was observed at the APM before IPR stimulation, consistent with the result of the subcellular fractionation analysis (Fig. 1*D*), it appeared to translocate from the APM to the cytosol after 30 min of stimulation. In addition, immunostaining signals of EPI64 unexpectedly increased in the cells after IPR stimulation (compare Fig. 5*A*, *panels a* and *g*). To confirm whether increased EPI64 signals were attributable to increased protein expression, a quantitative immunoblotting analysis was performed. As anticipated, up-regulation of EPI64 protein expression was clearly observed after IPR stimulation for 5–60 min (Fig. 5, *B* and *C*, *total panels*), and a ~2-fold increase in EPI64 protein expression was observed after stimulation for 60 min. The results of the subcellular fractionation analyses clearly showed that the amount of EPI64 protein at the APM and the cytosol was decreased and increased, respectively,

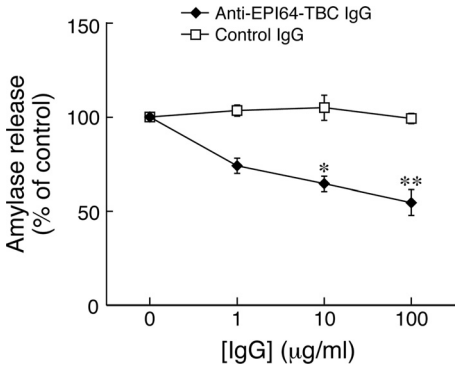

FIGURE 2. **Inhibition of amylase release by anti-EPI64-TBC IgG.** The effect of purified antibody against the TBC/Rab-GAP domain (anti-EPI64-TBC IgG) on IPR-induced amylase release from SLO-permeabilized parotid acinar cells was investigated as described under "Experimental Procedures." Amylase release is represented as the percentage of that without the antibody (means ± S.E. of four independent experiments, performed in triplicate). 100% amylase release corresponds to 5.80 ± 0.46% of the total amylase activity (100.1 ± 11.8 mg maltose/0.1 ml cell suspension). Data were analyzed by two-way ANOVA, followed by Williams' post hoc test. *, $p < 0.025$; **, $p < 0.005$. Note that the anti-EPI64-TBC IgG (*closed diamonds*) inhibited IPR-induced amylase release from SLO-permeabilized parotid acinar cells in a dose-dependent manner, whereas control rabbit IgG (*open squares*) had no effect.

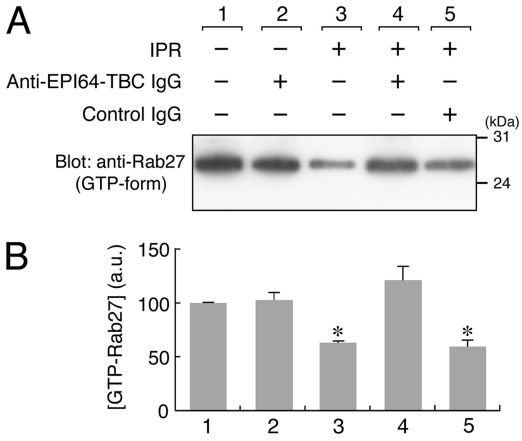

FIGURE 3. **Effect of anti-EPI64-TBC IgG on the GTP-binding status of Rab27.** The amount of GTP-Rab27 in SLO-permeabilized parotid acinar cells with or without anti-EPI64-TBC IgG treatment was measured using a GTP-Rab27 pull-down assay with GST-SHD. *A*, GTP-Rab27 trapped by GST-SHD was detected by immunoblotting using anti-Rab27 antibody. Typical data from five independent experiments are shown. *B*, intensity of Rab27 bands in *A* was measured. *Bars* indicate means ± S.E. of five independent experiments. *, $p < 0.01$ (Student's unpaired *t* test). Note that the amount of endogenous GTP-Rab27 was significantly decreased after IPR stimulation under control conditions (*lanes 3* and *5*), whereas such reduction was not observed in the presence of anti-EPI64-TBC IgG (*lane 4*). These results indicated that the anti-EPI64-TBC antibody inhibited the GTPase activity of Rab27, possibly through inhibition of Rab27-GAP activity of EPI64.

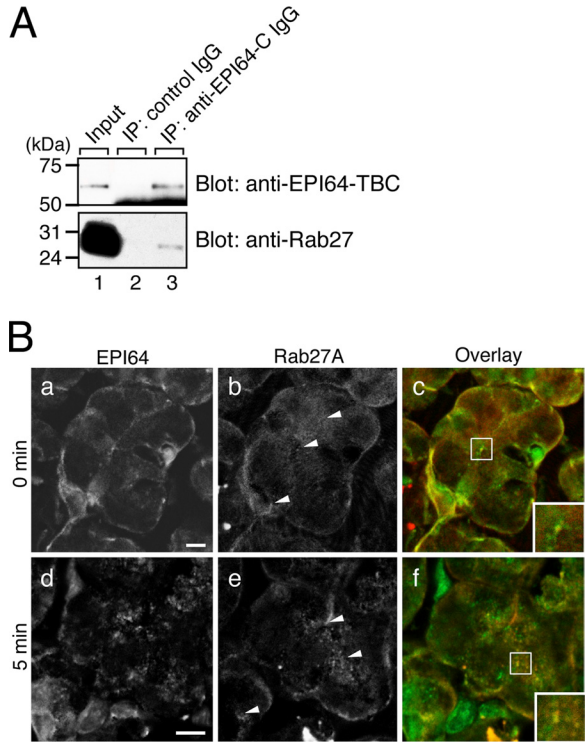

FIGURE 4. **Interaction between EPI64 and Rab27 in parotid acinar cells.** *A*, endogenous interaction between EPI64 and Rab27 as revealed by co-immunoprecipitation assays. Cell homogenate of 1 μg of protein was applied to lane 1. Immunoprecipitates with control rabbit IgG and anti-EPI64-C IgG were loaded on *lanes 2* and *3*, respectively. *B*, co-localization between EPI64 and Rab27A at the luminal sites of parotid acinar cells. Parotid gland slices were incubated without (*a–c*) and with 1 μM IPR for 5 min (*d–f*). Each section was co-immunostained with anti-EPI64-TBC antibody (*a* and *d*; *green*) and anti-Rab27A antibody (*b* and *e*; *red*). Merged images are shown in *c* and *f*. *Arrowheads* represent acinar luminal sites. The *insets* show magnified views of the *boxed area*. Scale bars, 5 μm.

after IPR stimulation (Fig. 5, *B* and *C*, *APM* and *Cyto panels*), indicating that EPI64 protein translocates from the APM to the cytosol.

Effect of IPR Stimulation on mRNA Expression of EPI64 in Parotid Acinar Cells—IPR-induced up-regulation of EPI64 protein expression may be caused by up-regulation of the *EPI64* mRNA level or by increased translational activity. To determine the primary cause of the up-regulation of EPI64 protein expression, IPR-induced gene expression of *EPI64* was quantified by real-time PCR (Fig. 6). *EPI64* mRNA expression was increased ~2-fold by IPR stimulation for 30 min, which closely corresponds to the 2-fold increase in EPI64 protein expression described above (Fig. 5*C*, *total panel*). Therefore, we concluded that IPR stimulation rapidly induced *EPI64* mRNA levels and consequently EPI64 protein levels.

Effects of Actinomycin D Treatment and Antisense Oligonucleotides on Expression of EPI64 and Amylase Release—Finally, we assessed whether up-regulation of EPI64 protein expression was essential for IPR-induced amylase release. Parotid acinar cells were treated with actinomycin D, an RNA synthesis inhibitor. In the presence of actinomycin D (50 μg/ml for 50 min), up-regulation of the level of both *EPI64* mRNA and EPI64 protein was completely abolished (Fig. 7, *A* and *B*, respectively). Interestingly, treatment of parotid acinar cells with actinomycin D inhibited IPR-induced amylase release to ~60% of that of the control cells (Fig. 7*C*). To rule out the possibility that actinomycin D suppressed the expression of genes other than *EPI64* that were essential for amylase release, we further tested the effect of *EPI64* antisense LNA on IPR-induced amylase release from SLO-permeabilized parotid acinar cells. The results showed that the antisense LNA significantly inhibited both up-regulation of *EPI64* mRNA/EPI64 protein (Fig. 7, *D* and *E*) and IPR-induced amylase release (Fig. 7*F*), suggesting that increased EPI64 protein after IPR stimulation also contributes to amylase release.

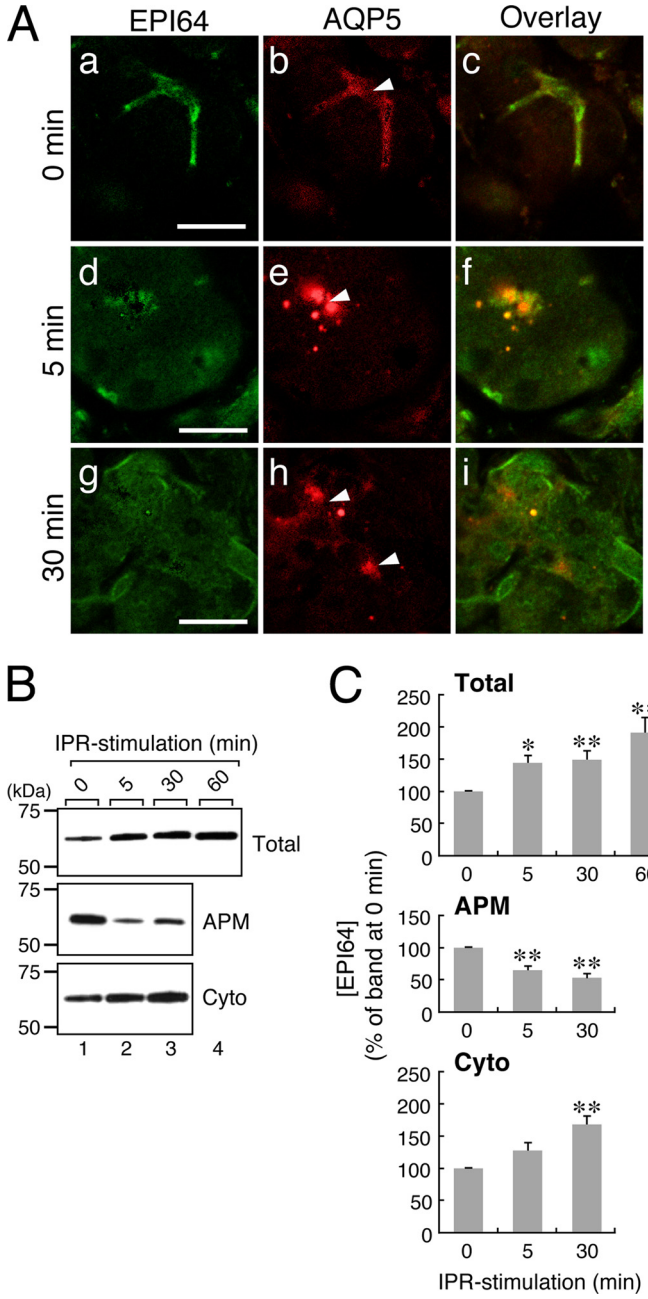

FIGURE 5. **Redistribution and increased protein expression of EPI64 in parotid acinar cells after IPR stimulation.** *A*, redistribution of EPI64 protein was observed after IPR stimulation by immunohistochemistry. Parotid gland slices were incubated with 1 μM IPR for 5 min or 30 min. Each section was co-immunostained with anti-EPI64-TBC antibody (*a*, *d*, and *g*; *green*) and anti-aquaporin 5 antibody (AQP5, an APM marker; *b*, *e*, and *h*; *red*). Merged images are shown in *c*, *f*, and *i*. *Arrowheads* represent acinar luminal sites. Scale bars, 5 μm. *B*, increased expression of EPI64 protein in parotid acinar cells after IPR stimulation as revealed by immunoblotting using anti-EPI64-C antibody (*Total panel*). Alteration of EPI64 protein in the APM fraction (*APM panel*) and cytosolic fraction (*Cyto panel*) was also demonstrated by using quantitative immunoblotting. Typical data from four independent experiments are shown. *C*, intensity of EPI64 bands in *B* was measured. Bars indicate means ± S.E. of four independent experiments. Data were analyzed by two-way ANOVA, followed by Williams' post hoc test. *, $p < 0.025$; **, $p < 0.005$.

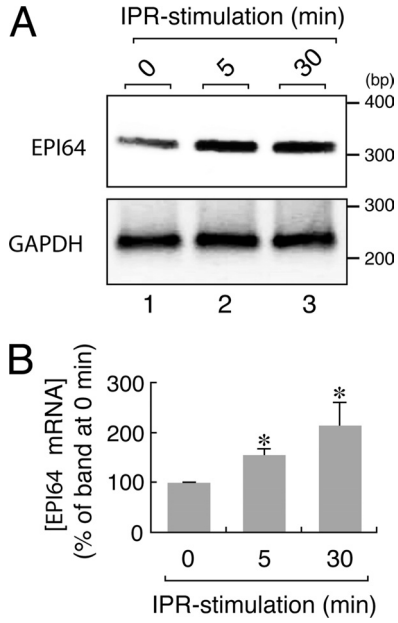

FIGURE 6. **Effect of IPR stimulation on the mRNA expression of *EPI64* in parotid acinar cells.** IPR stimulation-dependent increase in the level of *EPI64* mRNA as revealed by RT-PCR analysis (*A*) and real-time PCR analysis (*B*). The acinar cells were stimulated with 1 μM IPR for 5 or 30 min, and PCR analyses were performed as described under "Experimental Procedures." Typical data from four independent experiments are shown in *A*. The size of the molecular weight markers (*bp*, base pair) is shown at the *right* in *A*. Bars in *B* indicate means ± S.E. of four independent experiments. *, $p < 0.01$ (Student's unpaired *t* test). Note that *EPI64* mRNA expression was dramatically increased by IPR stimulation.

DISCUSSION

In a previous study, we identified EPI64 as a candidate Rab27-GAP because overexpression of EPI64, but not a catalytically inactive EPI64 mutant, in cultured melanocytes induced inactivation of endogenous Rab27A molecules, and EPI64 exhibited Rab27A-GAP activity *in vitro* (17). However, whether EPI64 actually functions as a physiological Rab27-GAP in secretory cells was not investigated. In the present study, we investigated the biological function of EPI64 and its regulatory mechanism in secretory vesicle exocytosis using rat parotid acinar cells as a secretion model, because these parotid acinar cells express both Rab27A/B and their effectors, Slac2-c, Slp4-a, and Noc2, and because they have been shown to participate in amylase release (22, 31, 37). We found that EPI64 was expressed endogenously in rat parotid acinar cells, and that it was enriched in the APM and less abundant in the cytosol of parotid acinar cells at rest (Fig. 1). We noted that EPI64 was not localized on the secretory granule membranes, where Rab27 is localized under resting conditions (31). Such APM-specific localization of EPI64, together with our previous observations of IPR stimulation-dependent redistribution of Rab27 (from secretory granules to the APM, and to the cytosol) (22), prompted us to hypothesize that EPI64 on the APM promotes the GTPase activity of Rab27, which is translocated from secretory granules to the APM after exocytosis. Moreover, we suggested that the inactivated GDP-Rab27 is released from the APM due to the function of a GDP dissociation inhibitor (22). This hypothesis was strongly supported by our finding that the introduction of an antibody against the TBC/Rab-GAP domain of EPI64 in SLO-permeabilized parotid acinar cells completely inhibited the stimulation-dependent reduction in GTP-Rab27 (Fig. 3). In addition, the redistribution of Rab27 in saponin-permeabilized parotid acinar cells (particularly the move from the APM to the

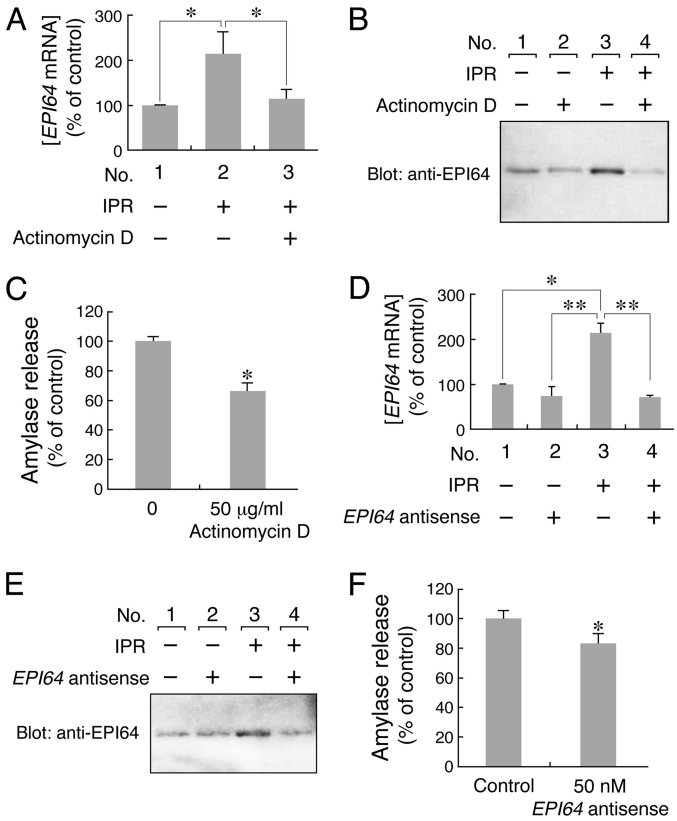

FIGURE 7. **Down-regulation of *EPI64* expression caused a significant reduction in the amount of amylase release from parotid acinar cells.** *A*, effect of actinomycin D, an RNA synthesis inhibitor, on mRNA expression of *EPI64*. Actinomycin D treatment and real-time PCR analyses were performed as described under "Experimental Procedures." The control is represented by *EPI64* mRNA expression of untreated parotid acinar cells. Bars indicate means ± S.E. of four independent experiments. *, $p < 0.01$ (Student's unpaired *t* test). *B*, effect of actinomycin D on the protein expression of EPI64 was investigated by immunoblotting with anti-EPI64-C antibody. Note that IPR stimulation-dependent up-regulation of EPI64 protein was completely inhibited by treatment with actinomycin D (*lane 4*). *C*, effect of actinomycin D on IPR-induced amylase release from parotid acinar cells was investigated. Parotid acinar cells were incubated with actinomycin D for 30 min and then stimulated with 1 μM IPR for 20 min. Amylase release is represented as the percentage of that without actinomycin D (means ± S.E. of four independent experiments, performed in duplicate). 100% amylase release corresponds to 5.45 ± 0.41% of the total amylase activity (60.7 ± 4.6 mg maltose/0.1 ml cell suspension). Data were analyzed by Student's unpaired *t* test. *, $p < 0.01$. Actinomycin D inhibited IPR-induced amylase release from parotid acinar cells. *D*, effect of *EPI64* antisense LNA on *EPI64* mRNA expression in parotid acinar cells. Antisense LNA treatment and real-time PCR analyses were performed as described under "Experimental Procedures." SLO-permeabilized parotid acinar cells were incubated with 50 nM antisense LNA for 20 min and then stimulated with 1 μM IPR for 30 min. The control is represented by *EPI64* mRNA expression of untreated parotid acinar cells. Bars indicate means ± S.E. of three independent experiments. Data were analyzed by Student's unpaired *t* test. *, $p < 0.05$. **, $p < 0.01$. *E*, effect of *EPI64* antisense LNA on the protein expression of EPI64 was investigated by immunoblotting with anti-EPI64-C antibody. Note that IPR stimulation-dependent up-regulation of EPI64 protein was also completely inhibited by treatment with *EPI64* antisense LNA (*lane 4*). *F*, effect of *EPI64* antisense LNA on IPR-induced amylase release from parotid acinar cells. Parotid acinar cells were incubated with 50 nM antisense LNA for 30 min and then stimulated with 1 μM IPR for 20 min. 100% amylase release corresponds to 3.44 ± 0.66% of the total amylase activity (52.6 ± 10.0 mg maltose/0.1 ml cell suspension). Data were analyzed by Student's unpaired *t* test. *, $p < 0.05$. Note that both *EPI64* mRNA/EPI64 protein expression and IPR-induced amylase release from the acinar cells were inhibited by *EPI64* antisense LNA.

cytosol) following IPR stimulation was inhibited by treatment with GTPγS, a non-hydrolyzable analog of GTP (supplemental Fig. S1). Therefore, the GTPase activity of Rab27 was likely to be required for dissociation of Rab27 from the APM. Although GAP is generally thought to be a negative regulator that terminates GTPase signaling, the anti-EPI64-TBC antibody attenuated IPR-induced amylase release in a dose-dependent manner (Fig. 2). This result may not be surprising in light of a recent report showing that the GTPase activity of Rab27 is not required for exocytosis itself in platelets, and that the GTPase activity of Rab27 occurs only after exocytosis (29). Therefore, we speculate that a Rab27 must undergo a proper GTP-GDP cycle for amylase release, and that inhibition of the cycle by the specific antibody, *i.e.* the accumulation of GTP-Rab27 on the APM, would inhibit amylase release by reducing the number of Rab27 molecules available to mediate the next round of exocytosis, preventing sustained amylase release.

Another important but unexpected finding was that both the *EPI64* mRNA level and EPI64 protein level were increased by stimulation with IPR (Figs. 5 and 6), and that suppression of increases in *EPI64* mRNA by actinomycin D or *EPI64* antisense LNA inhibited IPR-induced amylase release (Fig. 7). Currently, the exact mechanism by which IPR induced transcription of *EPI64* mRNA is unknown, but IPR stimulation is known to increase the cAMP level in parotid acinar cells as a result of activation of adenylate cyclase (28). Because a candidate CREB (cAMP response element-binding) protein binding site(s) (half site; TGACG) was identified in the human and mouse *TBC1D10A/EPI64* genes by the CREB Target Gene Database, it is highly possible that the transcription of *EPI64* mRNA was activated by CREB protein through protein kinase A (PKA) phosphorylation. In fact, *EPI64* mRNA expression was suppressed by the protein kinase A inhibitor 5–24 (supplemental Fig. S2). Because treatment of parotid acinar cells with *EPI64* antisense LNA significantly reduced the amount of amylase released, cytosolic EPI64 increase after IPR stimulation is also likely to regulate the biogenesis and/or recycling of secretory granules (*e.g.* transport of secretory granules to the apical region), in which Rab27 may be involved (42, 43). A proper GTP-GDP cycle of Rab27 is presumably required for these processes.

It has been very recently reported that members of the TBC1D10 family, including EPI64, function as GAPs for Rab35 (39, 40, 44), which is known to regulate a variety of cellular events, including recycling of T-cell receptor and oocyte yolk protein (40, 44, 45), cytokinesis (46), neurite outgrowth (47, 48), actin bundling (49, 50), and exosome secretion (39). However, Rab35 protein is expressed at very low levels in parotid acinar cells relative to those in the rat brain (supplemental Fig. S3*A*, *lane 6*), and we detected Rab35 in the SGM-rich fraction of parotid acinar cells (supplemental Fig. S3*A*, *lane 8*). The involvement of Rab35 in IPR-induced amylase release was also investigated by using a Rab35-specific trapper (GST-RBD35) that we have recently developed (30). However, GST-RBD35 had no effect on IPR-induced amylase release from SLO-permeabilized parotid acinar cells (supplemental Fig. S3*B*), in contrast to the inhibitory effect of GST-SHD, a Rab27-specific trapper, as previously reported (31), suggesting that Rab35 itself may not be directly involved in amylase secretion (51). Moreover, the level of endogenous GTP-Rab35 monitored by GST-RBD35 was increased by IPR stimulation (supplemental Fig. S3*C*, compare *lanes 2* and *5*), in contrast to the decreased level

of GTP-Rab27 (Fig. 3). However, since the addition of the anti-EPI64-TBC IgG into parotid acinar cells increased the amount of GTP-Rab35 regardless of the presence of IPR stimulation (supplemental Fig. S3*C*, *lanes 3* and *4*), EPI64 is also likely to function as a Rab35-GAP (39, 40, 44). Because the addition of the anti-EPI64-TBC IgG alone increased the amount of GTP-Rab35, but had no effect on the basal amylase secretion (data not shown), GTP-Rab35 is unlikely to be directly involved in amylase secretion. Rab35 may contribute to recycling of membrane proteins (*e.g.* β-adrenergic receptor) (40, 44, 45, 52) and/or biogenesis of new amylase-containing vesicles (53). Further extensive research is needed to determine the molecular mechanism by which EPI64 regulates two distinct small GTPases, Rab27 and Rab35, during amylase release from parotid acinar cells.

In summary, we have demonstrated that EPI64 protein enhanced the GTPase activity of Rab27 (and also Rab35) in parotid acinar cells, and that IPR-induced amylase release was regulated by EPI64 expression and Rab27-GAP activity. To our knowledge, this is the first report to demonstrate that endogenous EPI64 has Rab27-GAP activity under physiological conditions. EPI64 is expressed ubiquitously (15), and inactivation of Rab27 has been shown to occur after exocytosis in other secretory cells (29); therefore, we propose that EPI64 functions as a Rab27-GAP that regulates secretion events in a variety of secretory cells, similar to its role in parotid acinar cells. Our findings, together with previous reports on the function of EPI64 in microvillar formation (15) and in exosome secretion (39), indicate that EPI64 is a multifunctional protein that regulates Rab27/35 through its GAP activity and microvillar formation independent of its GAP activity (16).

Acknowledgments—We thank Dr. Takashi Itoh for preparing the anti-EPI64 antibodies and Megumi Aizawa for technical assistance.

REFERENCES

1. Zerial, M., and McBride, H. (2001) *Nat. Rev. Mol. Cell Biol.* **2,** 107–117
2. Pfeffer, S. R. (2001) *Trends Cell Biol.* **11,** 487–491
3. Fukuda, M. (2008) *Cell. Mol. Life Sci.* **65,** 2801–2813
4. Stenmark, H. (2009) *Nat. Rev. Mol. Cell Biol.* **10,** 513–525
5. Bock, J. B., Matern, H. T., Peden, A. A., and Scheller, R. H. (2001) *Nature* **409,** 839–841
6. Pereira-Leal, J. B., and Seabra, M. C. (2001) *J. Mol. Biol.* **313,** 889–901
7. Itoh, T., Satoh, M., Kanno, E., and Fukuda, M. (2006) *Genes Cells* **11,** 1023–1037
8. Seabra, M. C., and Wasmeier, C. (2004) *Curr. Opin. Cell Biol.* **16,** 451–457
9. Grosshans, B. L., Ortiz, D., and Novick, P. (2006) *Proc. Natl. Acad. Sci. U.S.A.* **103,** 11821–11827
10. Schwartz, S. L., Cao, C., Pylypenko, O., Rak, A., and Wandinger-Ness, A. (2007) *J. Cell Sci.* **120,** 3905–3910
11. Barr, F., and Lambright, D. G. (2010) *Curr. Opin. Cell Biol.* **22,** 461–470
12. Fukuda, M. (2011) *Biosci. Rep.* **31,** 159–168
13. Ishibashi, K., Kanno, E., Itoh, T., and Fukuda, M. (2009) *Genes Cells* **14,** 41–52
14. Fukuda, M. (2005) *J. Biochem.* **137,** 9–16
15. Reczek, D., and Bretscher, A. (2001) *J. Cell Biol.* **153,** 191–206
16. Hanono, A., Garbett, D., Reczek, D., Chambers, D. N., and Bretscher, A. (2006) *J. Cell Biol.* **175,** 803–813
17. Itoh, T., and Fukuda, M. (2006) *J. Biol. Chem.* **281,** 31823–31831
18. Fukuda, M., and Mikoshiba, K. (1999) *J. Biol. Chem.* **274,** 31428–31434
19. Fukuda, M., Kanno, E., and Yamamoto, A. (2004) *J. Biol. Chem.* **279,** 13065–13075
20. Fluiter, K., ten Asbroek, A. L. M. A., de Wissel, M. B., Jakobs, M. E., Wissenbach, M., Olsson, H., Olsen, O., Oerum, H., and Baas, F. (2003) *Nucleic Acids Res.* **31,** 953–962
21. Imai, A., Nashida, T., Yoshie, S., and Shimomura, H. (2003) *Arch. Oral Biol.* **48,** 597–604
22. Imai, A., Yoshie, S., Nashida, T., Fukuda, M., and Shimomura, H. (2009) *Eur. J. Oral Sci.* **117,** 224–230
23. Paul, E., Hurtubise, Y., and LeBel, D. (1992) *Membrane Biol.* **127,** 129–137
24. Turner, R. J., and Moran, A. (1982) *Am. J. Physiol.* **242,** F406–F414
25. Mizuno, M., Kameyama, Y., and Yokota, Y. (1991) *Biochim. Biophys. Acta* **1084,** 21–28
26. Imai, A., Nashida, T., and Shimomura, H. (2004) *Arch. Biochem. Biophys.* **422,** 175–182
27. Bernfeld, P. (1955) *Methods Enzymol.* **1,** 149–158
28. Takuma, T., and Ichida, T. (1988) *J. Biochem.* **103,** 95–98
29. Kondo, H., Shirakawa, R., Higashi, T., Kawato, M., Fukuda, M., Kita, T., and Horiuchi, H. (2006) *J. Biol. Chem.* **281,** 28657–28665
30. Fukuda, M., Kobayashi, H., Ishibashi, K., and Ohbayashi, N. (2011) *Cell Struct. Funct.* **36,** 155–170
31. Imai, A., Yoshie, S., Nashida, T., Shimomura, H., and Fukuda, M. (2004) *J. Cell Sci.* **117,** 1945–1953
32. Butcher, F. R., Goldman, J. A., and Nemerovski, M. (1975) *Biochim. Biophys. Acta* **392,** 82–94
33. Castle, D., and Castle, A. (1998) *Crit. Rev. Oral Biol. Med.* **9,** 4–22
34. Fujita-Yoshigaki, J. (1998) *Cell Signal.* **10,** 371–375
35. Kuroda, T. S., Fukuda, M., Ariga, H., and Mikoshiba, K. (2002) *J. Biol. Chem.* **277,** 9212–9218
36. Fukuda, M., Imai, A., Nashida, T., and Shimomura, H. (2005) *J. Biol. Chem.* **280,** 39175–39184
37. Imai, A., Yoshie, S., Nashida, T., Shimomura, H., and Fukuda, M. (2006) *Arch. Biochem. Biophys.* **455,** 127–135
38. Imai, A., Fukuda, M., Yoshie, S., Nashida, T., and Shimomura, H. (2009) *Arch. Oral Biol.* **54,** 361–368
39. Hsu, C., Morohashi, Y., Yoshimura, S., Manrique-Hoyos, N., Jung, S., Lauterbach, M. A., Bakhti, M., Grønborg, M., Möbius, W., Rhee, J., Barr, F. A., and Simons, M. (2010) *J. Cell Biol.* **189,** 223–232
40. Patino-Lopez, G., Dong, X., Ben-Aissa, K., Bernot, K. M., Itoh, T., Fukuda, M., Kruhlak, M. J., Samelson, L. E., and Shaw, S. (2008) *J. Biol. Chem.* **283,** 18323–18330
41. Matsuzaki, T., Suzuki, T., Koyama, H., Tanaka, S., and Takata, K. (1999) *Cell Tissue Res.* **295,** 513–521
42. Yu, E., Kanno, E., Choi, S., Sugimori, M., Moreira, J. E., Llinás, R. R., and Fukuda, M. (2008) *Proc. Natl. Acad. Sci. U.S.A.* **105,** 16003–16008
43. Ostrowski, M., Carmo, N. B., Krumeich, S., Fanget, I., Raposo, G., Savina, A., Moita, C. F., Schauer, K., Hume, A. N., Freitas, R. P., Goud, B., Benaroch, P., Hacohen, N., Fukuda, M., Desnos, C., Seabra, M. C., Darchen, F., Amigorena, S., Moita, L. F., and Thery, C. (2010) *Nature Cell Biol.* **12,** 19–30
44. Gao, Y., Balut, C. M., Bailey, M. A., Patino-Lopez, G., Shaw, S., and Devor, D. C. (2010) *J. Biol. Chem.* **285,** 17938–17953
45. Sato, M., Sato, K., Liou, W., Pant, S., Harada, A., and Grant, B. D. (2008) *EMBO J.* **27,** 1183–1196
46. Kouranti, I., Sachse, M., Arouche, N., Goud, B., and Echard, A. (2006) *Curr. Biol.* **16,** 1719–1725
47. Chevallier, J., Koop, C., Srivastava, A., Petrie, R. J., Lamarche-Vane, N., and Presley, J. F. (2009) *FEBS Lett.* **583,** 1096–1101
48. Kanno, E., Ishibashi, K., Kobayashi, H., Matsui, T., Ohbayashi, N., and Fukuda, M. (2010) *Traffic* **11,** 491–507
49. Zhang, J., Fonovic, M., Suyama, K., Bogyo, M., and Scott, M. P. (2009) *Science* **325,** 1250–1254
50. Shim, J., Lee, S. M., Lee, M. S., Yoon, J., Kweon, H. S., and Kim, Y. J. (2010) *Mol. Cell. Biol.* **30,** 1421–1433
51. Tsuboi, T., and Fukuda, M. (2006) *J. Cell Sci.* **119,** 2196–2203
52. Allaire, P. D., Marat, A. L., Dall'Armi, C., Di Paolo, G., McPherson, P. S., and Ritter, B. (2010) *Mol. Cell* **37,** 370–382
53. Uytterhoeven, V., Kuenen, S., Kasprowicz, J., Miskiewicz, K., and Verstreken, P. (2011) *Cell* **145,** 117–132